Cellular and Molecular Biology
E-ISSN : 1165-158X / P-ISSN : 0145-5680
www.cellmolbiol.org

Circ-PRMT5 stimulates the proliferative ability in Wilms' tumor through the miR-7-5p/KLF4 axis

Jing Zhang[1#], Yingyu Quan[2#], Xiaoxia Su[1], Baowei Qiu[1], Qi Dong[1*]

[1] Department of General Surgery, Hainan Women and Children's Medical Center, Haikou, China
[2] Department of Pediatrics, Hainan General Hospital Hainan Affiliated Hospital of Hainan Medical University, Haikou, China

# contributed equally to this work

ARTICLE INFO

Original paper

Article history:
Received: June 22, 2023
Accepted: August 20, 2023
Published: August 31, 2023

Keywords:

Circ-PRMT5, MiR-7-5p, KLF4, Wilms' tumor, proliferation

ABSTRACT

CircRNAs are extensively discovered in mammals and they are closely linked to tumor cell behaviors. This study aims to detect the expression pattern of circ-PRMT5 in Wilms' tumor and its ability in influencing tumor development. Circ-PRMT5 levels in Wilms' tumor samples were detected. The regulatory effect of circ-PRMT5 on proliferative ability in Wilms' tumor cells was assessed by cell counting kit-8 (CCK-8), colony formation and 5-Ethynyl-2'- deoxyuridine (EdU) assay. The interaction in the circ-PRMT5/miR-7-5p/KLF4 axis was determined by luciferase assay. Rescue experiments were conducted to reveal the role of the circ-PRMT5/miR-7-5p/KLF4 axis in Wilms' tumor development. Circ-PRMT5 was highly expressed in Wilms' tumor samples. High levels of circ-PRMT5 predicted advanced tumor staging in patients with Wilms' tumor. Knockdown of circ-PRMT5 markedly suppressed proliferative ability in Wilms' tumor cells. Luciferase assay confirmed the interaction in the circ-PRMT5/miR-7-5p/KLF4 axis. Rescue experiments finally identified that circ-PRMT5 stimulated the malignant development of Wilms' tumor by activating the miR-7-5p/KLF4 axis. Circ-PRMT5 is upregulated in Wilms' tumor samples, which is closely linked to its tumor staging. It stimulates proliferative ability in Wilms' tumor cells by activating the miR-7-5p/KLF4 axis.

Doi: http://dx.doi.org/10.14715/cmb/2023.69.8.36

Introduction

Wilms' tumor, also known as nephroblastoma, is the most common malignant tumor of the genitourinary system that originates in the kidney. It predominantly affects pediatric patients, accounting for approximately 6% of all pediatric malignancies (1-3). Wilms' tumor is relatively rare, with an estimated incidence of 0.01% in children younger than 15 years (1, 2). The average age of diagnosis for Wilms' tumor is around 36 months, and it rarely occurs in individuals older than 10 years or younger than 6 months (1, 2).

The exact causes and mechanisms underlying the development of Wilms' tumor remain largely unknown. However, it is widely believed that the tumor originates from the abnormal proliferation of postrenal embryonic nephrons (4, 5). Pathologically, Wilms' tumor is classified into several histological types, including blastema, mesenchyme, epithelium, and mixed types. The presence of anaplastic cells within the tumor plays a crucial role in determining the prognosis and clinical outcome of Wilms' tumor (5).

Clinical symptoms of Wilms' tumor are often atypical and vary depending on the stage and location of the tumor. The most common presentation is the presence of an asymptomatic abdominal mass. Other manifestations may include hematuria (blood in the urine), abdominal pain, hypertension (high blood pressure), and symptoms caused by the compression of adjacent structures by the tumor mass. Wilms' tumor can also be associated with multiple congenital malformations, further complicating its diagnosis and management (6, 7).

The therapeutic strategy for Wilms' tumor aims to prevent complications and ultimately reduce mortality rates (8-10). Early diagnosis is crucial for successful treatment, and it is essential to identify the pathological subtype of the tumor to develop individualized treatment approaches (4, 8, 11, 12).

In recent years, non-coding RNAs (ncRNAs) have emerged as important regulators of gene expression and are known to play significant roles in various biological processes. These ncRNAs can negatively regulate gene transcription or induce degradation of downstream messenger RNAs (mRNAs) through complementary base pairing, thereby influencing cellular behaviors (13, 14). With the advent of high-throughput sequencing and microarray analysis, several classes of ncRNAs, such as long non-coding RNAs (lncRNAs) and microRNAs (miRNAs), have been identified as potential biomarkers and key players in tumorigenesis (15, 16).

In addition to lncRNAs and miRNAs, circular RNAs (circRNAs) have gained significant attention as a novel class of ncRNAs with potential regulatory functions (17, 18). CircRNAs are characterized by a covalently closed loop structure and are more stable compared to linear RNAs due to their resistance to exonucleases. These unique features make circRNAs promising candidates for

* Corresponding author. Email: dqearth@163.com

diagnostic and therapeutic applications in cancer.

Previous studies have shed light on the potential role of circ-PRMT5, a circular RNA, in cancer progression (19, 20). In the context of Wilms' tumor, our previous work analyzed differentially expressed circRNAs in Wilms' tumor samples, and circ-PRMT5 was found to be significantly upregulated. Given its dysregulation in Wilms' tumor, we aim to investigate the functional role of circ-PRMT5 in the development of Wilms' tumor and elucidate its underlying molecular mechanisms.

In this study, we present a comprehensive analysis of circ-PRMT5 in Wilms' tumor, exploring its potential involvement in tumor pathogenesis. By examining its expression patterns and functional implications, we seek to contribute to a better understanding of the molecular mechanisms driving Wilms' tumor development and identify potential therapeutic targets. Our findings may provide valuable insights into the diagnosis, prognosis, and treatment strategies for Wilms' tumor, ultimately improving patient outcomes in this pediatric malignancy.

Materials and Methods

Patients and Wilms' tumor samples

Paired Wilms' tumor and paracancerous tissues were surgically resected from 45 patients (22 males and 23 females) with Wilms' tumor. The average age of included patients was 25.5 months. None of them had preoperative treatment. Samples were independently confirmed by two experienced pathologists. This study got approval from Ethics Committee of Hainan Women and Children's Medical Center and was conducted after informed consent.

Cell culture

Human Wilms' tumor cell lines (HFWT, WT-CLS1 and 17-94) were first collected and digested from fresh Wilms'tumor tissues, and one renal tubular epithelial cell line (HK-2) was purchased from American Type Culture Collection (ATCC) (Manassas, VA, USA). All cells were cultured in Dulbecco's modified eagle medium (DMEM) (Gibco, Rockville, MD, USA) with 10% fetal bovine serum (FBS) (Gibco, Rockville, MD, USA), 100 U/mL penicillin and 100 μg/mL streptomycin in a 5% CO_2 incubator at 37°C. Cell passage was conducted until cells were grown to 80-90% confluence.

Transfection

Transfection plasmids were purchased from GenePharma (Shanghai, China). Cells were grown to 30-50% and transfected using Lipofectamine 2000 (Invitrogen, Carlsbad, CA, USA). Transfected cells for 48 h were utilized for *in vitro* experiments.

Cell proliferation assay

Cells were inoculated in a 96-well plate with 2×10^3 cells per well. At the appointed time points, the absorbance value at 490 nm of each sample was recorded using the cell counting kit-8 (CCK-8) kit (Dojindo Laboratories, Kumamoto, Japan) for plotting the viability curves.

Colony formation assay

Cells were inoculated in a 6-well plate with 200 cells per well and cultured for 2 weeks. The culture medium was replaced once in the first week and twice in the second week. Visible colonies were washed in phosphate-buffered saline (PBS), fixed in methanol for 20 min and dyed in 0.1% crystal violet for 20 min, which were finally captured and calculated.

5-Ethynyl-2'-deoxyuridine (EdU) assay

Cells were inoculated in a 24-well plate with 2×10^4 cells per well. They were incubated in 4% methanol for 30 min, followed by 10-min permeabilization in 0.5% TritonX-100 (Solarbio, Beijing, China), and 30-min reaction in 400 μL of 1×ApollorR. Afterward, cells were dyed in 4',6-diamidino-2-phenylindole (DAPI) for another 30 min. EdU-positive cells and DAPI-labeled nuclei were captured (Sigma-Aldrich, St. Louis, MO, USA).

Quantitative real-time polymerase chain reaction (qRT-PCR)

Extracted RNAs by TRIzol reagent (Invitrogen, Carlsbad, CA, USA) were reversely transcribed into complementary deoxyribose nucleic acids (cDNAs) using Primescript RT Reagent (TaKaRa, Otsu, Japan). The obtained cDNAs underwent qRT-PCR using SYBR®Premix Ex Taq™ (TaKaRa, Otsu, Japan). Glyceraldehyde 3-phosphate dehydrogenase (GAPDH) and U6 were the internal references. Each sample was performed in triplicate, and the relative level was calculated by $2^{-\Delta\Delta Ct}$. The primer sequences were shown below: circ-PRMT5: Forward: 5'-ATCGTGCTGCCTTTCAGTTT-3', Reverse: 5'-GGTCACGCGGATCTGATACT-3'; KLF4: Forward: 5'-CCCCACCTTCTTCACCCCTAGA-3', Reverse: 5'-GTAAGGTTTCTCACCTGTGTGGG-3'; GAPDH: Forward: 5'-CAAGGTCAT CCATGACAACTTTG-3', Reverse: 5'-GTCCACCACCCTGTTGCTGTAG-3'; MiR-7-5p: Forward: 5'-CCACGTTGGAAGACTAG-TGATTT-3', Reverse: 5'-TATGGTTGTTCTGCTCTC-TGTCTC-3'; U6: Forward: 5'-CTCGCTTCGGCAGCA-CA-3', Reverse: 5'-AACGCTTCACGAATTTGCGT-3'

Western blot

Cells were lysed for isolating cellular protein and electrophoresed. Protein samples were loaded on polyvinylidene fluoride (PVDF) membranes (Millipore, Billerica, MA, USA). Subsequently, non-specific antigens were blocked in 5% skim milk for 2 hours. Membranes were reacted with primary and secondary antibodies for the indicated time. Band exposure and analyses were finally conducted.

Luciferase assay

Cells inoculated in 24-well plates were co-transfected with NC mimic/miR-7-5p mimic and wild-type/mutant-type vector, respectively. 48 hours later, cells were lysed for measuring luciferase activity (Promega, Madison, WI, USA).

Statistical analysis

GraphPad Prism 5 V5.01 (La Jolla, CA, USA) was used for data analyses. Data were expressed as mean ± standard deviation. Differences between groups were analyzed by the *t*-test. The chi-square test was used for analyzing the relationship between circ-PRMT5 level and clinical characteristics of patients with Wilms' tumor. The Pearson correlation test was applied for assessing the correlation between the two expressions. $P<0.05$ was considered sta-

tistically significant.

Results

Circ-PRMT5 was highly expressed in Wilms' tumor samples

Differential expression of circ-PRMT5 was detected in 45 paired Wilms tumor samples. Compared with paracancerous tissues, circ-PRMT5 was highly expressed in Wilms' tumor tissues (Figure 1A). Similarly, circ-PRMT5 was also upregulated in Wilms' tumor cells (Figure 1B). Based on the median level of circ-PRMT5 in the included 45 patients, they were assigned into the high and low-level groups, respectively. As analyzed data showed, circ-PRMT5 level was correlated to tumor staging in patients with Wilms' tumor (Table 1).

Circ-PRMT5 promoted proliferative potential in Wilms' tumor

The transfection efficacy of sh-circ-PRMT5 was excellent in both HFWT and 17-94 cells (Figure 2A). Knockdown of circ-PRMT5 remarkably decreased viability (Figure 2B), colony number (Figure 2C) and EdU-positive rate (Figure 2D) in HFWT and 17-94 cells. It is indicated that circ-PRMT5 promoted proliferative potential in Wilms' tumor cells.

Circ-PRMT5 regulated miR-7-5p/KLF4 axis in Wilms' tumor

Bioinformatics analysis showed binding sequences in the 3'UTR of circ-PRMT5 and miR-7-5p. Binding sequences were also identified in the 3'UTR of miR-7-5p and KLF4 (Figure 3A). Overexpression of miR-7-5p decreased luciferase activity in wild-type circ-PRMT5 or wild-type KLF4 vector. However, luciferase activities in mutant-type vectors were unchangeable (Figure 3B, 3C). Thus, we confirmed the interaction in the circ-PRMT5/miR-7-5p/KLF4 axis. In Wilms' tumor cells, transfection of sh-circ-PRMT5 upregulated miR-7-5p (Figure 3D). The protein level of KLF4 was downregulated after the silence of circ-PRMT5 (Figure 3E). Moreover, we verified that circ-PRMT5 was negatively correlated to miR-7-5p level, and miR-7-5p level was negatively correlated to KLF4 level in Wilms' tumor samples (Figure 3F, 3G).

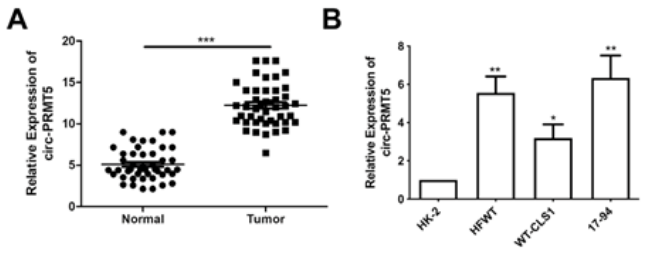

Figure 1. Circ-PRMT5 was highly expressed in Wilms' tumor samples. Differential expression of circ-PRMT5 in Wilms' tumor samples and paracancerous ones (A). Circ-PRMT5 level in Wilms' tumor cell lines (B). Data were expressed as mean±SD. **P*<0.05, ***P*<0.01, ****P*<0.001.

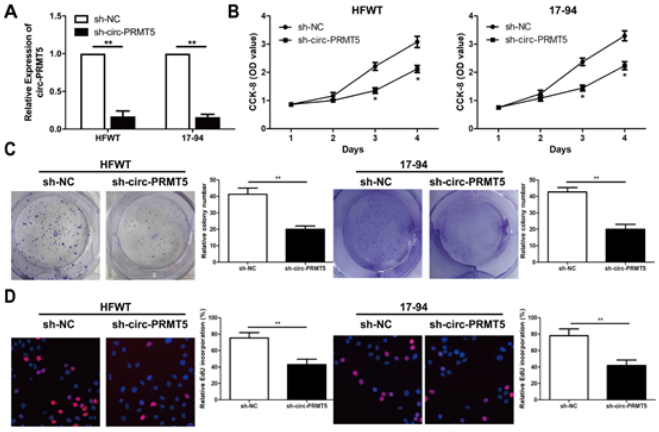

Figure 2. Circ-PRMT5 promoted proliferative potential in Wilms' tumor. Transfection efficacy of sh-circ-PRMT5 in HFWT and 17-94 cells (A). Viability in HFWT and 17-94 cells transfected with sh-NC or sh-circ-PRMT5 (B). Colony number in HFWT and 17-94 cells transfected with sh-NC or sh-circ-PRMT5 (magnification 10×) (C). EdU-positive rate in HFWT and 17-94 cells transfected with sh-NC or sh-circ-PRMT5 (magnification 40×) (D). Data were expressed as mean±SD. **P*<0.05.

KLF4 was involved in the regulation of Wilms' tumor proliferation

To further uncover the relationship between circ-PRMT5 and the miR-7-5p/KLF4 axis, rescue experiments

Table 1. Association of circ-PRMT5 expression with clinicopathologic characteristics of Wilms' tumor.

Parameters	Number of cases	circ-PRMT5 expression		*P*-value
		Low (n=23)	High (n=22)	
Age (months)				0.256
<24	29	13	16	
≥24	16	10	6	
Gender				0.465
Male	27	15	12	
Female	18	8	10	
T stage				0.016
T1-T2	32	20	12	
T3-T4	13	3	10	
Lymph node metastasis				0.652
No	22	12	10	
Yes	23	11	12	

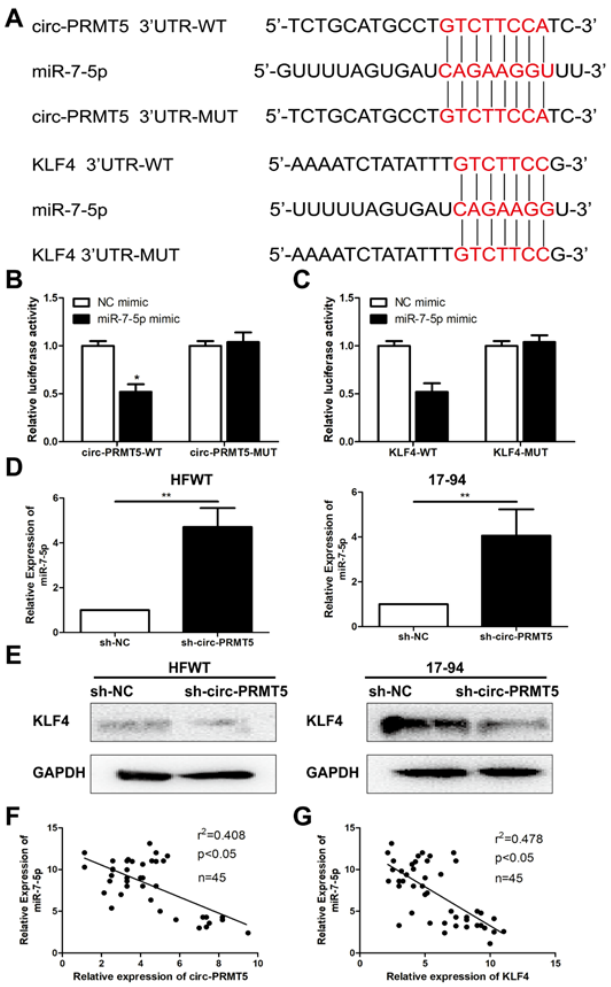

Figure 3. Circ-PRMT5 regulated miR-7-5p/KLF4 axis in Wilms' tumor. Binding sequences in the 3'UTR of circ-PRMT5, miR-7-5p and KLF4 (A). Luciferase activity in cells co-transfected with NC mimic/miR-7-5p mimic and circ-PRMT5-WT/circ-PRMT5-MUT, respectively (B). Luciferase activity in cells co-transfected with NC mimic/miR-7-5p mimic and KLF4-WT/KLF4-MUT, respectively (C). MiR-7-5p level in HFWT and 17-94 cells transfected with sh-NC or sh-circ-PRMT5 (D). Protein level of KLF4 in HFWT and 17-94 cells transfected with sh-NC or sh-circ-PRMT5 (E). A negative correlation between expression levels of circ-PRMT5 and miR-7-5p in Wilms' tumor samples (F). A negative correlation between expression levels of miR-7-5p and KLF4 in Wilms' tumor samples (G). Data were expressed as mean±SD. **P*<0.05, ***P*<0.01.

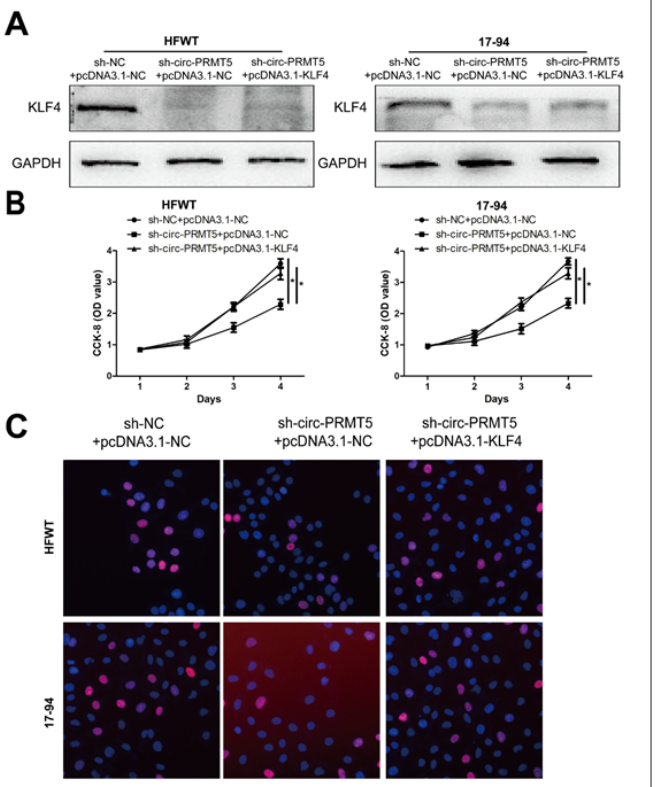

Figure 4. KLF4 was involved in the regulation of Wilms' tumor proliferation. Protein level of KLF4 in co-transfected HFWT and 17-94 cells (A). Viability in co-transfected HFWT and 17-94 cells (magnification 10×) (B). EdU-positive rate in co-transfected HFWT and 17-94 cells (magnification 40×) (C). Data were expressed as mean±SD. **P*<0.05, ***P* < 0.01.

were conducted. The transfection efficacy of pcDNA-KLF4 was first tested in HFWT and 17-94 cells (Figure 4A). Interestingly, decreased viability (Figure 4B) and EdU-positive rate (Figure 4C) in Wilms' tumor cells with circ-PRMT5 knockdown were partially reversed by overexpression of KLF4.

Discussion

Traditional treatment for Wilms' tumor is aggressive, which not only induces severe adverse events but also influences the normal development of the body (6-8). About 25% of survivors develop chronic diseases after 25 years of diagnosis or adulthood, including renal failure, congestive heart failure, pulmonary fibrosis, kyphosis, infertility, secondary tumor, etc. (8,9). Wilms' tumor severely affects children health and their families owing to the low survival rate (8-11). It is urgent to clarify the pathogenesis and etiology of Wilms' tumor (11,12). Therapeutic efficacy and prognosis in patients with Wilms' tumor vary a lot because of individualized differences, suggesting the vital role of genetic variation in the development of Wilms' tumor (5-10). Screening of susceptible populations and exploration of molecular genetic mechanisms in Wilms' tumor are of great significance (4, 8, 11, 12).

Differentially expressed circRNAs in different tissues, cell lines and pathological stages have been highlighted (17,18). CircRNAs are featured by the closed loop structure, displaying more resistance to RNases and other exonucleases than linear RNAs (18). Because of the great conservation, stability and differential expressions, circRNAs are promising tumor hallmarks (16,18). It is reported that circ-PRMT5 is abnormally expressed in tumor samples and linked to prognosis (17,18). In this paper, circ-PRMT5 was upregulated in Wilms' tumor samples. Knockdown of circ-PRMT5 reduced viability, colony number and EdU-positive rate in Wilms' tumor cells, suggesting the suppressed proliferative potential.

Functionally, circRNAs exert their biological roles by sponging corresponding miRNAs as multiple upstream MREs exist (21-24). Bioinformatics analysis predicted binding sequences in the 3'UTR of circ-PRMT5 and miR-7-5p. KLF4 also had shared sequences with that of miR-7-5p. As our experimental evidences showed, miR-7-5p was confirmed to be the target binding circ-PRMT5, while KLF4 was the downstream gene of miR-7-5p. Moreover, circ-PRMT5 level was negatively correlated to miR-7-5p level and positively correlated to KLF4 level. Interestingly, KLF4 was able to reverse the regulatory effect of circ-

PRMT5 on proliferative potential in Wilms' tumor cells. It is concluded that circ-PRMT5 stimulated proliferative potential in Wilms' tumor by activating the miR-7-5p/KLF4 axis.

The present study provided significant insights into the molecular mechanisms underlying Wilms' tumor development and progression. The study demonstrated that circ-PRMT5, a circular RNA, is upregulated in Wilms' tumor samples and exhibits a close association with tumor staging. Through a series of comprehensive experiments and analyses, the researchers reveal that circ-PRMT5 plays a crucial role in stimulating the proliferative ability of Wilms' tumor cells. Specifically, it exerts its influence by activating the miR-7-5p/KLF4 axis, a regulatory pathway involved in cell proliferation and differentiation. This finding adds to the growing body of evidence highlighting the importance of non-coding RNAs, such as circular RNAs, in modulating gene expression and contributing to cancer development. The identification of the miR-7-5p/KLF4 axis as a downstream target of circ-PRMT5 provides a deeper understanding of the specific molecular interactions involved in Wilms' tumor pathogenesis. By delineating this regulatory pathway, the study opens up avenues for further research and potential therapeutic interventions targeting circ-PRMT5 and its downstream effectors. Moreover, these findings have clinical implications, as circ-PRMT5 could serve as a potential biomarker for Wilms' tumor diagnosis, prognosis, and therapeutic response. The upregulation of circ-PRMT5 in tumor samples suggests its potential as a diagnostic indicator, while its association with tumor staging underscores its relevance for prognostic stratification. Furthermore, targeting circ-PRMT5 or the miR-7-5p/KLF4 axis could offer novel therapeutic strategies for inhibiting tumor growth and improving patient outcomes.

In summary, this study uncovers the functional role of circ-PRMT5 in Wilms' tumor and highlights its involvement in the regulation of the miR-7-5p/KLF4 axis. The findings shed light on the complex molecular mechanisms underlying Wilms' tumor pathogenesis and provide valuable insights that can inform future research and clinical approaches in the field of pediatric oncology.

Ethical compliance

This study got approval from the Ethics Committee of Hainan Women and Children's Medical Center and was conducted after informed consent.

Conflict of interest

The authors declared no conflict of interest.

Acknowledgements

This work was supported by the project supported by Hainan Province Clinical Medical Center QWYH202175).

References

1. Ghamdi DA, Bakshi N, Akhtar M. Teratoid Wilms Tumor: Report of Three Cases and Review of the Literature. Turk J Pathol 2019; 35(1): 61-68.
2. Nuriding H, Wang X, Shen Y, Liu Y, Yan M. Fos-Related Antigen 1 May Cause Wnt-Fzd Signaling Pathway-Related Nephroblastoma in Children. J Biomed Nanotechnol 2022; 18(2): 527-534.
3. Leslie SW, Sajjad H, Murphy PB. Wilms Tumor (Nephroblastoma). 2020:
4. Treger TD, Chowdhury T, Pritchard-Jones K, Behjati S. The genetic changes of Wilms tumour. Nat Rev Nephrol 2019; 15(4): 240-251.
5. Cao MM, Huang CP, Wang YF, Ma DM. Extrarenal Wilms' Tumor of the Female Genital System: A Case Report and Literature Review. Chin Med Sci J 2017; 32(4): 274-278.
6. Leung RS, Liesner R, Brock P. Coagulopathy as a presenting feature of Wilms tumour. Eur J Pediatr 2004; 163(7): 369-373.
7. Beckwith JB, Zuppan CE, Browning NG, Moksness J, Breslow NE. Histological analysis of aggressiveness and responsiveness in Wilms' tumor. Med Pediatr Oncol 1996; 27(5): 422-428.
8. Phelps HM, Kaviany S, Borinstein SC, Lovvorn HR. Biological Drivers of Wilms Tumor Prognosis and Treatment. Children-Basel 2018; 5(11):
9. Servaes SE, Hoffer FA, Smith EA, Khanna G. Imaging of Wilms tumor: an update. Pediatr Radiol 2019; 49(11): 1441-1452.
10. Oostveen RM, Pritchard-Jones K. Pharmacotherapeutic Management of Wilms Tumor: An Update. Pediatr Drugs 2019; 21(1): 1-13.
11. Lopes RI, Lorenzo A. Recent advances in the management of Wilms' tumor. F1000Res 2017; 6: 670.
12. Cone EB, Dalton SS, Van Noord M, Tracy ET, Rice HE, Routh JC. Biomarkers for Wilms Tumor: A Systematic Review. J Urology 2016; 196(5): 1530-1535.
13. Slack FJ, Chinnaiyan AM. The Role of Non-coding RNAs in Oncology. Cell 2019; 179(5): 1033-1055.
14. Ning B, Yu D, Yu AM. Advances and challenges in studying noncoding RNA regulation of drug metabolism and development of RNA therapeutics. Biochem Pharmacol 2019; 169(113638.
15. Wang M, Jiang S, Yu F, Zhou L, Wang K. Noncoding RNAs as Molecular Targets of Resveratrol Underlying Its Anticancer Effects. J Agr Food Chem 2019; 67(17): 4709-4719.
16. Finotti A, Fabbri E, Lampronti I, Gasparello J, Borgatti M, Gambari R. MicroRNAs and Long Non-coding RNAs in Genetic Diseases. Mol Diagn Ther 2019; 23(2): 155-171.
17. Dong R, Ma XK, Chen LL, Yang L. Increased complexity of circRNA expression during species evolution. Rna Biol 2017; 14(8): 1064-1074.
18. Li D, Li Z, Yang Y, et al. Circular RNAs as biomarkers and therapeutic targets in environmental chemical exposure-related diseases. Environ Res 2020; 180(108825.
19. Wang Y, Li Y, He H, Wang F. Circular RNA circ-PRMT5 facilitates non-small cell lung cancer proliferation through upregulating EZH2 via sponging miR-377/382/498. Gene 2019; 720(144099.
20. Du W, Li D, Guo X, et al. Circ-PRMT5 promotes gastric cancer progression by sponging miR-145 and miR-1304 to upregulate MYC. Artif Cell Nanomed B 2019; 47(1): 4120-4130.
21. Chen X, Huang J, Peng Y, Han Y, Wang X, Tu C. The role of circRNA polyribonucleotide nucleoside transferase 1 on gestational diabetes mellitus. Cell Mol Biol 2022; 68(6): 148-154.
22. Zhang C, Wu D, Wu Y, et al. CircRNA02318 Exerts Therapeutic Effects on Myocardial Ischemia-Reperfusion Injury Rats by Regulating the Nox1/Akt Through Inhibiting Drebrin. J Biomed Nanotechnol 2022; 18(12): 2794-2803.
23. Zang J, Lu D, Xu A. The interaction of circRNAs and RNA binding proteins: An important part of circRNA maintenance and function. J Neurosci Res 2020; 98(1): 87-97.
24. Li J, Li X, Qiao X. Analysis of circRNA regulatory network in myocardial tissue of type 1 diabetic mice. Cell Mol Biol 2021; 67(3): 201-203.